Scientific Research Publishing

Advances in Remote Sensing, 2025, 14(3), 170-187
https://www.scirp.org/journal/ars
ISSN Online: 2169-2688
ISSN Print: 2169-267X

Hydrological Variability in the Yaéré Floodplain (1984-2024): A Landsat-Based Remote Sensing Study of Surface Water Dynamics under Climate Change

Steven Chouto[1,2*], Elisabeth Fita Dassou[3], Sylvain Aoudou Doua[2], Bernard Gonne[4], Nathalie Annavaï[4], Thierry C. Fotso-Nguemo[1], Bruno Kolaouna-Labara[5]

[1]Climate Change Research Laboratory (CCRL), National Institute of Cartography, Yaounde, Cameroon
[2]Department of Geography, Faculty of Arts, Letters and Social Sciences, University of Maroua, Maroua, Cameroon
[3]Department of Meteorology and Hydrology, The National Advanced School of Engineering of Maroua, The University of Maroua, Maroua, Cameroon
[4]Department of Geography, Higher Teacher Training College, University of Maroua, Maroua, Cameroon
[5]Maroua Regional Agricultural Research Center, Institute of Agricultural Research for Development, Maroua, Cameroon
Email: *stevenchouto@gmail.com

How to cite this paper: Chouto, S., Fita Dassou, E., Aoudou Doua, S., Gonne, B., Annavaï, N., Fotso-Nguemo, T.C. and Kolaouna-Labara, B. (2025) Hydrological Variability in the Yaéré Floodplain (1984-2024): A Landsat-Based Remote Sensing Study of Surface Water Dynamics under Climate Change. *Advances in Remote Sensing*, **14**, 170-187.
https://doi.org/10.4236/ars.2025.143011

Received: July 2, 2025
Accepted: September 22, 2025
Published: September 25, 2025

Abstract

The Yaéré floodplain, located in the Logone watershed south of Lake Chad, is highly vulnerable to recurrent flooding that threatens local populations and the regional economy. This study quantifies the floodplain's hydrological dynamics over a 40-year period (1984-2024) by analysing 683 cloud-free Landsat images to map surface water changes. The results reveal substantial hydrological variability, with flooded areas ranging from complete absence (0 km^2) to a record maximum of 17,559 km^2 in October 2022, and an average flooded extent of approximately 1630 km^2. Flooding exhibits a pronounced seasonal pattern, peaking mainly in September and October, corresponding to key rainfall periods and river inflows critical for ecosystem functioning. Strong interannual variability is evident, contrasting exceptionally wet years such as 1999, 2022, and 2024 with notably dry periods including 1984, 1987, and 2007. Since 2019, a discernible increase in extreme flood events suggests intensifying precipitation trends consistent with regional climate change. Anthropogenic factors also shape the flood regime, notably the Maga dam and associated dykes constructed in the 1970s, which have modified natural inundation patterns and downstream hydrology. Diachronic mapping of flooded zones provides an essential tool for identifying areas of significant hydrological change, supporting targeted ecological restoration and risk management efforts. These findings offer critical insights for adaptive management of this vulnerable wet-

land in a changing climate. Integrating this remote sensing data into local and regional policy frameworks can enhance flood forecasting and early warning systems, improving community resilience to extreme hydrological events. Ultimately, this study contributes to the sustainable management of water resources and flood risk reduction in the Lake Chad basin, fostering more effective responses to future climatic uncertainties.

Keywords

Remote Sensing, Surface Water Dynamics, Flooding, Climate Variability, Yaéré

1. Introduction

Wetlands represent essential components of socio-ecological systems, due to their role in hydrological regulation and flood attenuation [1] [2]. Although widely recognised, this buffering function demonstrates considerable spatial and functional heterogeneity depending on the location, geomorphological structure, and hydrodynamic processes of each wetland type [3] [4]. Acting as transitional zones between aquatic and terrestrial environments, wetlands possess the ability to absorb, temporarily retain, and gradually release surplus water generated by rainfall events. Floodplains, in particular, stand out for their capacity to mitigate flood peaks, a phenomenon extensively documented in the scientific literature across diverse geographical settings [5]-[8]. By decelerating water flow and dispersing discharge volumes, these environments contribute significantly to downstream flood risk reduction.

Nevertheless, such regulatory capacity is neither uniform nor guaranteed: certain upstream wetlands, under specific hydrological conditions, may exacerbate flood risks by rapidly releasing stored water [3] [9]. These findings underscore the need to conceptualise wetlands not as uniform hydrological infrastructures, but as complex ecological systems whose flood-regulating functions are shaped by geomorphological, climatic, and anthropogenic factors [10]-[12]. Accordingly, regular hydrological monitoring and in-depth functional assessments of wetlands are essential prerequisites for informing integrated and place-based flood risk management policies.

The Yaéré floodplain, located in the Logone River basin at the south of Lake Chad, is a key wetland area supporting farming, fishing, and pastoral activities in the Sahel region [13]-[15]. This area is regularly affected by floods from the Logone River, which pose both risks to local communities and challenges for the regional economy [16]-[18]. In this environment, the connection between river dynamics and climate is central, given the complex nature of the local hydrology [14] [19]-[22].

The Logone River follows an annual flood cycle. It usually overflows in October, at the end of the rainy season, then the water recedes between November and Jan-

uary, leaving behind dry land with flooded depressions [4] [23] [24]. Each year, large areas are flooded, while only marshy zones remain above water, used for seasonal grazing. The extent and timing of flooding change from year to year, depending on rainfall and river flow. Before 1982, seasonal floods reached wide areas on the river's left bank, including parts of Waza National Park [25]. Local fishers, farmers, and herders used the land throughout the year based on a regular seasonal rhythm [26] [27]. However, in the late 1970s, a 30 km dam was built to create Lake Maga (400 km^2) for rice farming. This dam and its dykes reduced the natural floods in the Waza-Logone plain, causing environmental degradation and social disruption over about 800,000 hectares downstream between 1981 and the mid-1990s [28] [29]. Many studies have looked at flood and water recession cycles, as well as irrigation and water management. But recent changes in flood patterns have been observed. These changes are linked to both climate variations and human-built water infrastructure [13] [20] [24] [30]. Understanding how surface water behaves over time and space is now essential. It helps support better water management and prepares for the effects of changing climate and land use. This is especially important to predict how often and how strongly floods happen, and to assess how local communities can remain resilient.

Nowadays, tools exist that make it possible to overcome data and storage constraints. Google Earth Engine (GEE) provides access to the entire Landsat collection, covering more than 50 years of satellite observations, with images that are updated regularly [31]. This makes it possible to analyse long-term changes in surface water, spot seasonal or decadal patterns, and quickly detect unusual events such as drying or flooding. GEE is therefore a powerful platform for monitoring water resources, understanding environmental changes, and supporting sustainable land and water management. Most importantly, it helps track long-term trends, which is key to studying hydrological variability [32]. In this study, satellite data from Landsat missions covering four decades (1984 to 2024) were used. Analysis of the time series enables permanent and seasonal water bodies to be identified, as well as assessing changes in their extent over time. This approach provides an in-depth view of hydrological trends and interannual variations in the floodplain.

2. Study Area

The study focuses on the Waza-Logone floodplain, located in the Far North region of Cameroon. It is geographically bounded by latitude 12.4349747 in the north, 10.1511406 in the south, and by longitude 16.1315356 in the east and 14.0330922 in the west. This area matches the coverage of Landsat scene WRS 184/52. The plain stretches from the Yagoua-Limani dunes in the south-west to the town of Kousseri in the north-east (**Figure 1**). It takes its name from the overflows of the River Logone, fed by both river flooding and seasonal rainfall, the latter generally beginning in July. It is a major wetland ecosystem for several months each year, with a water level varying between 0.7 and 1.2 m [23]. The plain is located on the southern fringe of the Sahelian zone and is characterised by a rainfall pattern that

decreases from south to north, with annual rainfall varying between 600 and 750 mm. The rainy season usually runs from May/June to September/October, although its duration and intensity can fluctuate greatly from one year to the next. Outside this period, rainfall is rare or non-existent.

3. Data and Methods

3.1. Landsat Satellite Data

To analyse the extension of surface water in the Yaéré floodplain over the period 1982-2024, a series of optical satellite images from the Landsat program were processed using the Google Earth Engine (GEE) cloud-based platform. The study relied on data from five successive sensors: Landsat 4 TM, Landsat 5 TM, Landsat 7 ETM+, Landsat 8 OLI, and Landsat 9 OLI.

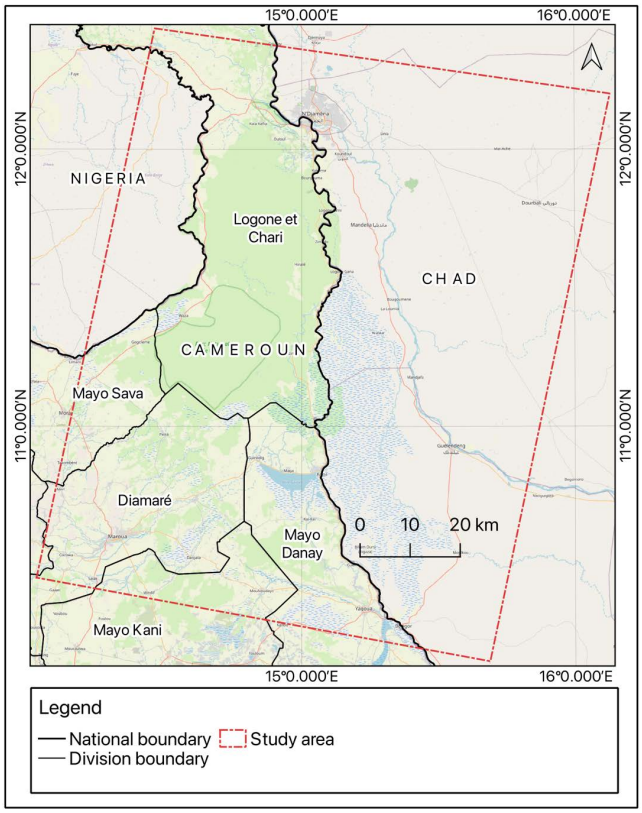

Figure 1. Location of study area. The map was produced by authors, with a background map from OSM (2025), administrative boundaries from GADM maps and data (2018-2022 GADM) and Landsat WRS 2 Descending Path Row.

In order to ensure data reliability and comparability over time, only Tier 1 images, pre-processed to Level 2 surface reflectance, were selected. The spatial extent of the study area was matched to the Landsat scene defined by path/row WRS 184/52 (**Figure 1**), ensuring full coverage of the floodplain. This methodological framework made it possible to maintain both temporal continuity and spatial consistency throughout the dataset, despite the technical evolution of the sensors across dec-

ades. A summary of the Landsat collections used is provided in Table 1:

Table 1. Landsat collections used in this study.

Satellite	Period	GEE Collection ID	Sensor(s)
Landsat 4	22 Aug. 1982-24 Jun. 1993	LANDSAT/LT04/C02/T1_L2	MSS/TM
Landsat 5	16 Mar. 1984-5 May 2012	LANDSAT/LT05/C02/T1_L2	TM
Landsat 7	28 May 1999-19 Jan. 2024	LANDSAT/LE07/C02/T1_L2	ETM+
Landsat 8	18 Mar. 2013-21 Apr. 2025	LANDSAT/LC08/C02/T1_L2	OLI/TIRS
Landsat 9	31 Oct. 2021-27 Apr. 2025	LANDSAT/LC09/C02/T1_L2	OLI-2/TIRS-2

3.2. Methodology

3.2.1. Delineation of Flooded Areas

The satellite images were pre-processed through several key steps to ensure data quality and consistency across the entire study period. Multitemporal Landsat scenes were selected, prioritizing those with less than 40% cloud cover. The pre-processing chain began with the spatial filtering of the WRS 184/52 path, followed by the application of the CFMASK algorithm to detect and mask clouds, cirrus, and cloud shadows using the blue band and a safety buffer. All optical and thermal bands were radiometrically scaled using sensor-specific coefficients to enable inter-sensor comparability. For Landsat 7 ETM+ images acquired after May 31, 2003 (when the Scan Line Corrector (SLC) failed), a temporal gap-filling method was applied using adjacent acquisitions within a ±32-day window.

To ensure spatial uniformity, all images were reprojected into the UTM Zone 33N (WGS84) coordinate system. The harmonization of spectral bands across the Landsat missions further facilitated the integration of observations over time. These preparatory steps ensured robust time series analyses from 1982 to 2024, mitigating sensor-related inconsistencies and atmospheric contamination. All data processing was implemented within the Google Earth Engine environment, taking advantage of its cloud computing capabilities for efficient handling of the high temporal and spatial resolution datasets.

Flood mapping was based on the spectral properties of surface water in the short-wave infrared (SWIR) domain. The SWIR2 band was selected as the primary indicator of soil moisture and surface water presence, owing to water's strong absorption characteristics at these wavelengths. A reflectance threshold of 0.08 was adopted. This threshold-based method was used to create binary maps for each image scene (1 = water, 0 = non-water). This binary classification approach, inspired by [17] [21] [33], enabled the generation of flood extent maps for each scene. These outputs were then aggregated to compute annual flood dynamics across the observation period.

3.2.2. Statistical Analysis of Flood Extents

Surface water dynamics across the Yaéré floodplain were assessed using a multi-temporal series of binary water masks derived from Landsat imagery between

1984 and 2024. For each year, the maximum and minimum extents of surface water were extracted, along with the corresponding dates of occurrence. The average annual surface water extent was also computed, providing a reference baseline for typical hydrological conditions over the four-decade period. The amplitude between yearly minima and maxima allowed for the characterisation of intra-annual variability, while years with exceptionally high or low averages were flagged as indicators of extreme flood or drought conditions.

To evaluate long-term hydrological variability, the standard deviation of annual extents was calculated, capturing interannual fluctuations in flood dynamics. The analysis thus provides a robust basis for understanding floodplain behaviour and for identifying hydrological anomalies, which is essential for flood risk management and climate impact assessments in semi-arid river basins.

3.2.3. Analysis of Rainfall Influence on Surface Water Dynamics

To explore the influence of rainfall on surface water extent, CHIRPS (Climate Hazards Group InfraRed Precipitation with Station data) daily rainfall data were used [34]. These data offer high-resolution (0.05˚) global coverage and were processed using GEE. The dataset was filtered to match the study period and clipped to the Logone basin boundary. Daily precipitation values were summed to calculate annual totals. Precipitation values were aggregated at the monthly scale and compared to monthly average surface water extents over selected hydrological years, notably 1984 and 2022. Basin-wide statistics were computed using zonal reduction functions to assess spatial coherence and interannual rainfall variability.

To quantify the strength and timing of rainfall's influence on surface water dynamics, Pearson correlation coefficients were first calculated between precipitation and water extent. Simple linear regression models were then fitted to estimate the marginal effect of rainfall on flood extent. To account for potential lagged hydrological responses, a time-lagged correlation analysis was performed, examining associations between surface water and preceding rainfall totals up to 30 days. This approach enabled the identification of delayed flood responses to rainfall events and contributed to a better understanding of rainfall-runoff dynamics in the floodplain context

4. Results

The availability of Landsat satellite imagery over the study area (WRS tile 184/52) has evolved significantly between 1984 and 2024 (**Figure 2**). Initial observations were limited, with 20 usable images from Landsat 5 (1984-1999) and only 2 from Landsat 4 (1987-1988). A temporal gap followed, before the launch of Landsat 7 in 1999, which became the main source of data with 336 images acquired through to 2024. Data availability increased notably from 2013 onwards with the introduction of Landsat 8 (256 images), and further improved with Landsat 9 (69 images since 2021). These recent missions have contributed to a denser temporal coverage, particularly suited for monitoring seasonal and interannual hydrological dy-

namics in the Yaéré floodplain. In total, 683 quality-filtered images were analysed, providing a robust temporal archive for detecting surface water changes and understanding long-term flood patterns in the region.

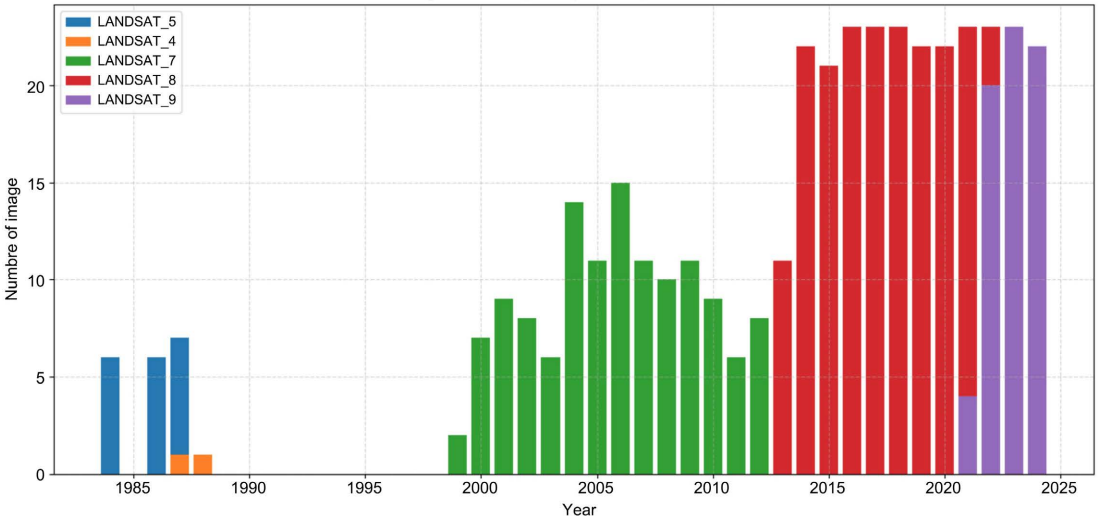

Figure 2. Temporal availability of Landsat satellite data (WRS 184/52) by sensor and by year (1984-2024). The figure illustrates the number of usable images per year from each sensor (Landsat 4, 5, 7, 8, and 9), highlighting a clear increase in acquisition frequency over time. Three phases can be observed: limited coverage during the early missions (Landsat 4 and 5), improved regularity with Landsat 7 (1999-2012), and a marked rise in image availability from 2013 onwards with the launch of Landsat 8 and later Landsat 9. This enhanced temporal resolution significantly strengthens the capacity to monitor seasonal and interannual flood dynamics in the Yaéré floodplain.

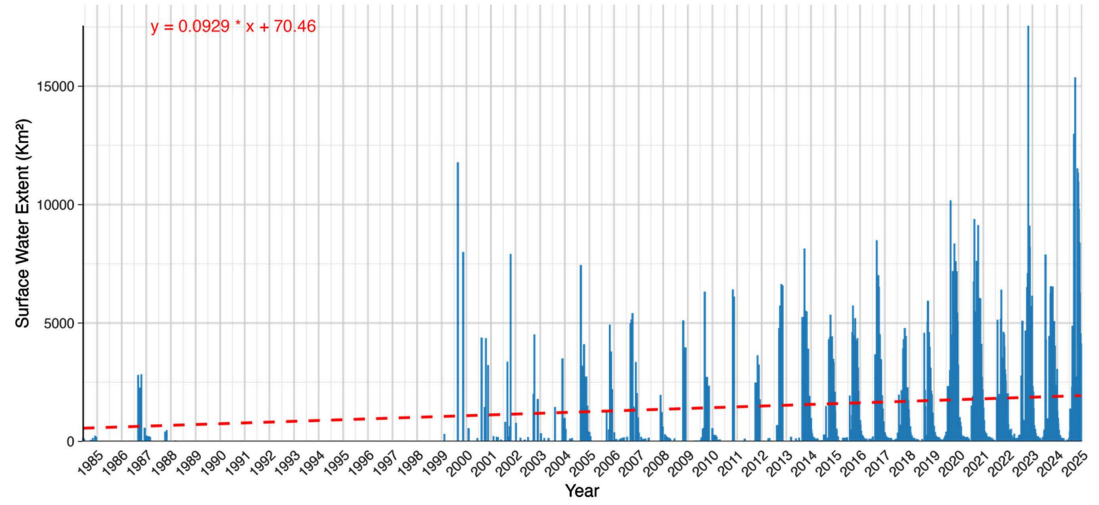

Figure 3. Evolution of surface water extent in the Yaéré floodplain (1984-2024).

The remote sensing analysis of Landsat imagery from 1984 to 2024 has made it possible to characterise, with precision, the long-term hydrological dynamics of the Yaéré floodplain over four decades. The spatial extent of surface water displays pronounced interannual variability, reflecting the complex interactions between rainfall patterns, river discharge, and floodplain topography. This variability

ranges from a complete absence of detectable surface water (0 km^2 recorded on 29 March 1987) to a historical maximum extent of 17,559.01 km^2 observed on 31 October 2022 (Figure 3). These fluctuations illustrate the irregular nature of flooding in the region and highlight the importance of long-term monitoring for understanding hydrological extremes and their implications for land use, ecosystems, and local livelihoods.

The above chart illustrates the marked variability in surface water extent over the 40-year study period. This considerable amplitude bears witness to the hydrological dynamics of this floodplain, with an average water surface area over the entire period of 1630.25 km^2. The years 1999, 2012, 2019, 2020, 2022 and 2024 stand out for their particularly high annual averages (in excess of 2000 km^2), while the years 1984, 1987, 1988 and 2007 show much lower values (less than 500 km^2). This contrast reflects the influence of climatic fluctuations on the hydrological regime of the Yaéré. The standard deviation associated with each year also highlights the extent of intra-annual variations, with particularly high values for 2022 (3487 km^2) and 2024 (4208 km^2), reflecting hydrological cycles marked by great contrasts. The general trend over the study period suggests a gradual increase in the average surface area under water, particularly since 2019, although this trend is punctuated by significant fluctuations.

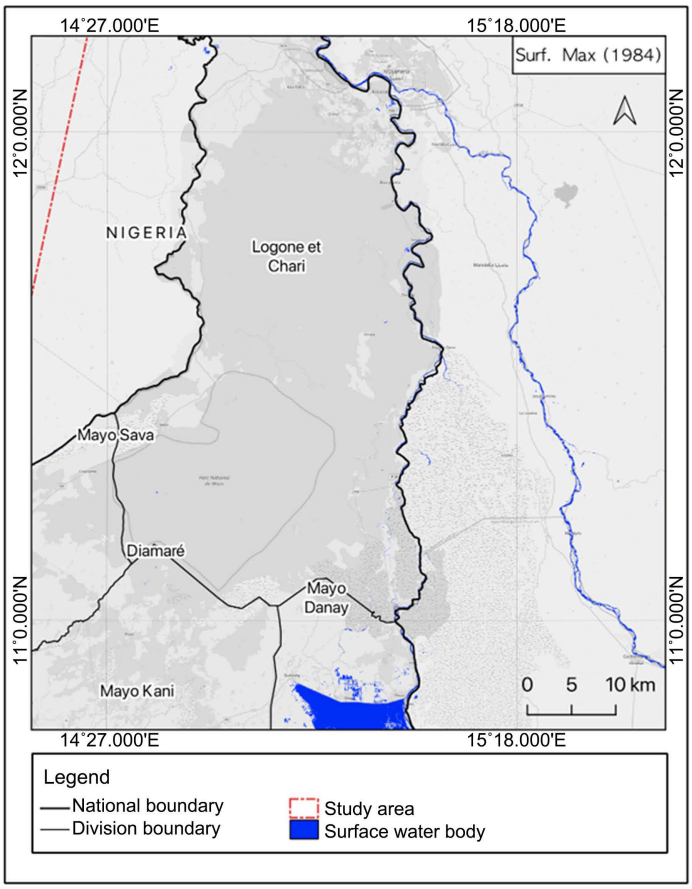

(a)

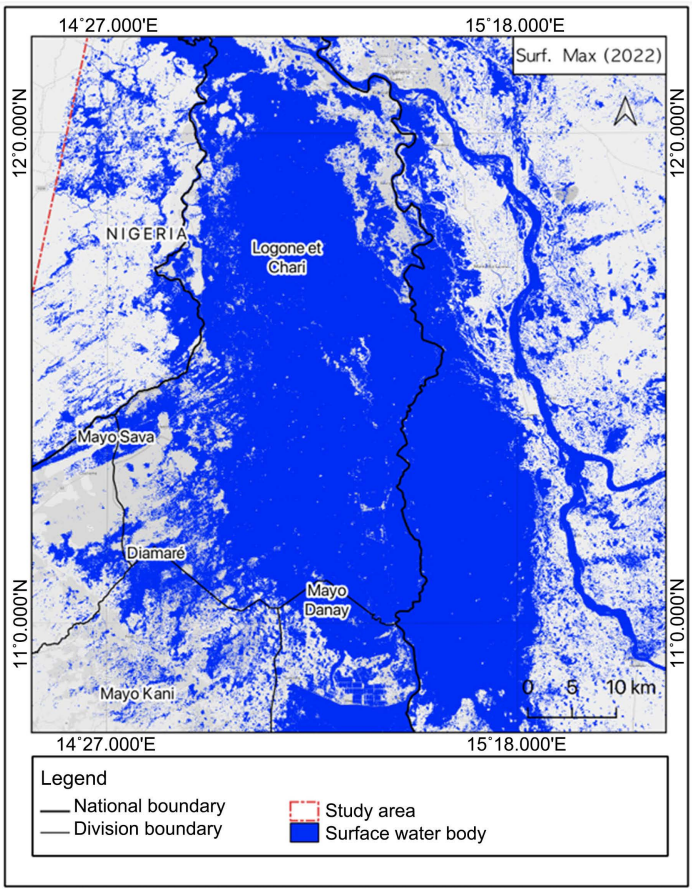

(b)

Figure 4. Maximum surface water extent in an extremely dry year (1984) and an extremely wet year (2022).

The results obtained show that flood-prone areas are subject to rainfall dynamics (**Figure 4(a)** and **Figure 4(b)**). In fact, the heavy rainfall in 2012 generated significant runoff, causing the flooding observed in the Yaéré. The Logone and Chari rivers have completely burst their banks. On the other hand, in 1984, as a result of the worsening climate, the Yaéré suffered severe stress, with little or no water surface area.

The spatial comparison between an extremely dry year (1984) and an exceptionally wet year (2022) highlights the high sensitivity of the Yaéré floodplain to hydrometeorological conditions (**Figure 4(a)** and **Figure 4(b)**). In 2022, following above-average rainfall and strong river discharge, both the Logone and Chari rivers overflowed their banks, resulting in widespread flooding across the entire floodplain. Surface water coverage extended far beyond the river channels, inundating low-lying areas and depressions over a vast spatial extent. In contrast, the 1984 image shows minimal surface water presence, reflecting the severe hydrological stress linked to ongoing drought conditions during that period. The floodplain appears almost entirely desiccated, with only a few residual water bodies detectable. These contrasting hydrological situations illustrate the strong depend-

ence of flood dynamics on seasonal rainfall input and river inflows. They also underscore the importance of long-term monitoring to capture extreme events at both ends of the hydrological spectrum.

Changes in hydrological dynamics can also be observed on a decadal scale. The 1984-1988 period, characterised by limited satellite coverage, shows relatively low average water surface areas (151.99 km^2 in 1984, 40.38 km^2 in 1988), with the notable exception of 1986 (average of 1749.58 km^2). The years 1999-2012 show alternating wet and dry periods, with peaks of 11,793.34 km^2 (1999) and 7920.22 km^2 (2001). The recent period (2013-2024), which benefits from a much higher density of observations thanks to the Landsat 8 and 9 satellites, reveals flooding events of exceptional magnitude, particularly in 2022 (maximum of 17,559.01 km^2) and 2024 (maximum of 15,372.07 km^2). This observation raises the question of the impact of climate change on the intensification of extreme hydrological phenomena in the region, although the improved temporal resolution of the observations must be taken into account when interpreting this trend.

The monthly distribution of peak surface water extent confirms the strong seasonality of flooding in the Yaéré floodplain (Figure 5). The majority of hydrological maxima are concentrated in the months of October (40%) and September (23.3%), which together account for nearly two-thirds of all observed flood peaks. These months correspond to the culmination of the rainy season and the period of maximum overflow from the Logone River. Secondary peaks occur in August (13.3%) and November (13.3%), reflecting the transitional phase of the flood cycle. Notably, March, July, and December each register 3.3% of flood peaks, suggesting the existence of exceptional hydrological events, potentially linked to abnormal rainfall or man-made changes to the regional hydrological system.

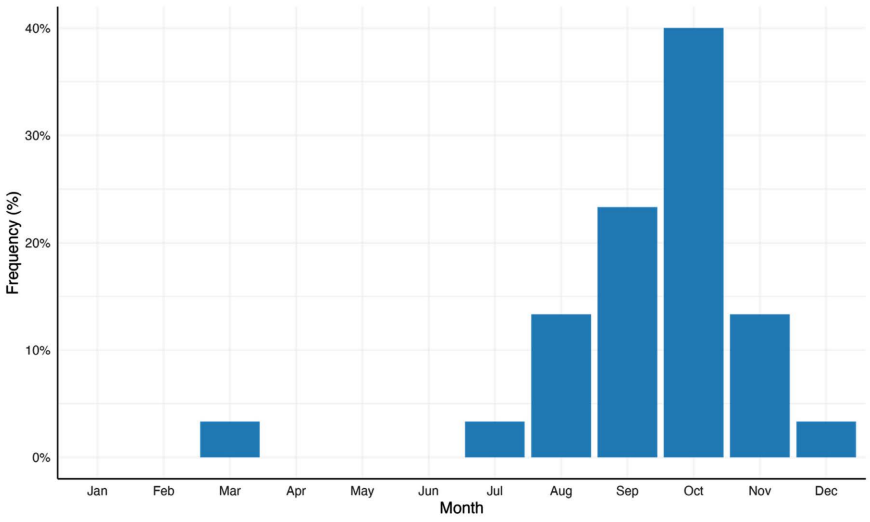

Figure 5. Frequency of monthly peak surface water extent (1984-2024).

To better understand the long-term trends in flooding within the Yaéré floodplain, Figure 6 presents the annual mean surface water extent over the 1984-2024

period, highlighting both variability and overarching patterns in flood dynamics.

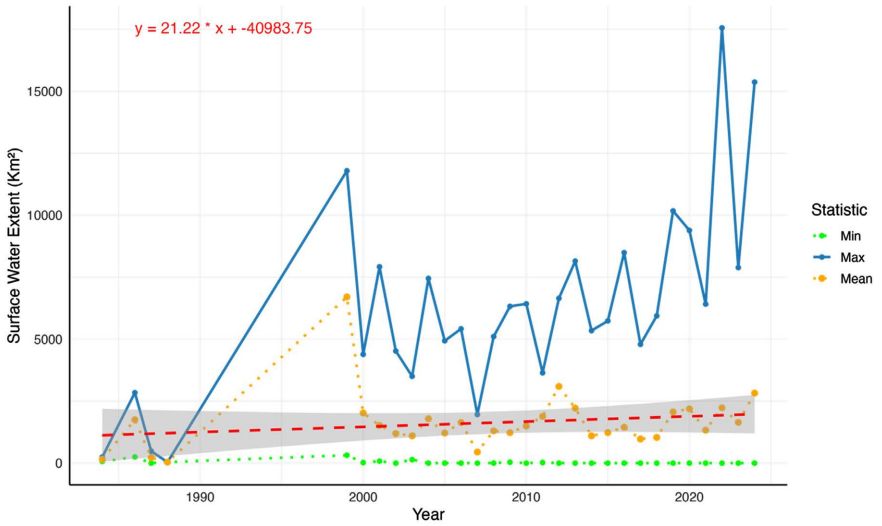

Figure 6. Annual mean surface water extent (1984-2024).

The above figure illustrates the annual fluctuations in surface water extent within the Yaéré floodplain over four decades. The data reveal significant inter-annual variability, with periods of both drought and exceptional flooding clearly identifiable. Notably, the years around 1999-2000 and those following 2019 stand out for elevated average surface water extents, while prolonged dry spells are reflected in consistently low minimum values. Extreme flood events are apparent in the peaks of maximum extents, emphasizing the floodplain's sensitivity to episodic hydrological surges. Over the entire period, there is a discernible upward trend in average flooded area, suggesting a gradual shift in the hydrological regime. However, this trend is accompanied by considerable year-to-year fluctuations, indicative of the complex interplay between climatic variability, potential land-use changes, and hydrological processes. The confidence interval surrounding the trend underscores greater uncertainty in the earliest and latest years, likely due to variable data availability and heightened hydrological extremes.

This observed long-term variability and recent increase in surface water extent in the Yaéré floodplain call for a deeper investigation into the underlying climatic drivers. Understanding how rainfall patterns, temperature fluctuations, and broader climate trends influence flood dynamics is essential to contextualise these hydrological changes. The following figure (**Figure 7**) explores the role of regional precipitation variability and its temporal distribution, aiming to link climatic factors with the observed flood regime shifts.

Inter-seasonal variations in surface areas follow a relatively regular cycle, with a gradual expansion of flooded areas during the rainy season (June-September), generally peaking between September and November, followed by a phase of receding water that begins in December and lasts until the end of the dry season or hydrological year. The intra-annual variation in water surfaces for the 2022-2023

hydrological year, for example (Figure 7), illustrates the expansion of floodable surfaces linked to rainfall between April and September. On closer examination, the low contribution of rainfall to surface area expansion conceals a more complex hydrological dynamic. As the rainfall increases, the surface area covered by water increases until September, causing material damage and loss of life in surplus years. From October onwards, the Logone and Chari rivers overflow into the Yaéré plain. The excess water then spills over into this gently sloping area, resulting in a considerable extension of the surface area occupied by water. As a result, the area flooded expands and river flooding occurs.

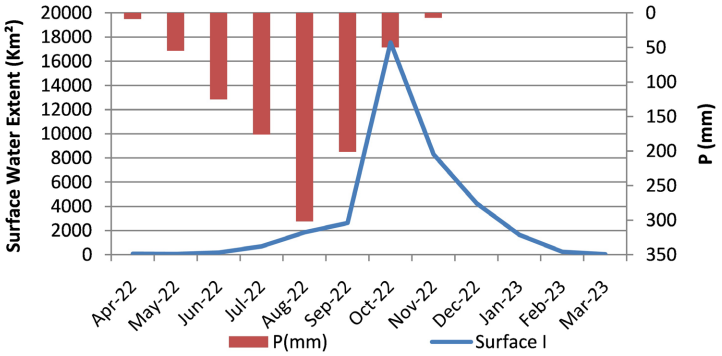

Figure 7. Relation between monthly rainfall and surface water water extent (1984-2024).

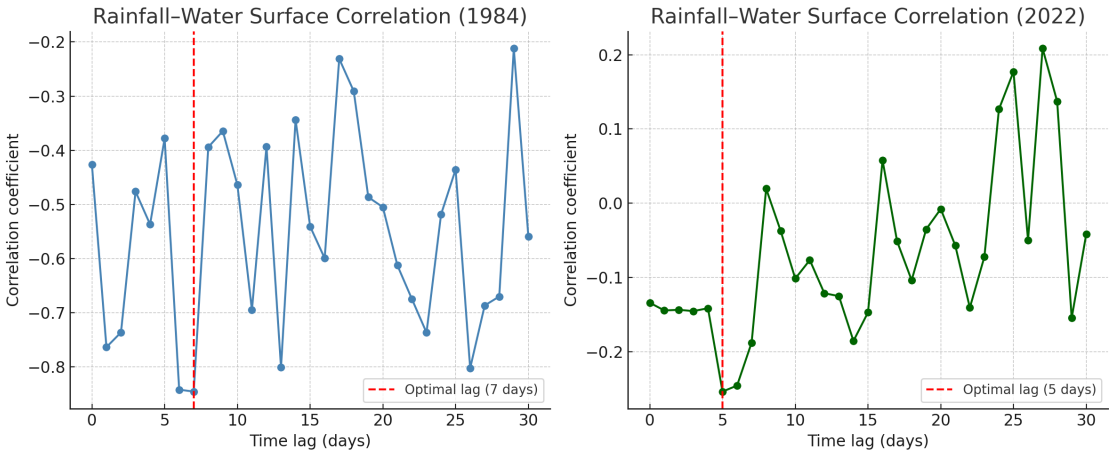

Figure 8. Relationship between rainfall and water surface area as a function of time lag for 1984 and 2022.

In addition to the hydrological dynamics previously described, the statistical analysis of the relationship between rainfall and flood extent reveals interannual variability in correlation strength. In 1984, a strong and statistically significant negative correlation was observed ($r = -0.99$, $p < 0.01$) between monthly rainfall and flooded surface area, with an optimal time lag of 7 days. This suggests a direct and immediate response of surface water to rainfall inputs, likely reflecting limited fluvial influence that year and a dominant role of local precipitation in driving flood expansion. In contrast, the year 2022 exhibited a much weaker and statistically insignificant correlation ($r = -0.20$, $p = 0.53$), with an optimal lag of 5 days

(Figure 8). This weak association aligns with hydrological observations indicating that most flooding resulted from fluvial overflows beginning in October, while peak rainfall occurred earlier, in August and September.

5. Discussion

5.1. Methodological Considerations and Limitations of the Study

The mapping of water surfaces in the Yaéré over the period 1984-2024 presents a number of methodological challenges that need to be discussed if the results are to be interpreted rigorously. The main limitation concerns the temporal heterogeneity of the Landsat image corpus analysed. Indeed, the continuity of observations is not ensured in a homogeneous manner over the entire study period, particularly during the 1990s when a significant gap was observed in the satellite archives. This discontinuity is mainly due to the limited availability of images with less than 40% cloud cover, the critical threshold used in our methodological protocol to guarantee the reliability of water surface detections. The region's climate, characterised by a marked rainy season, generates heavy cloud cover, which frequently makes it difficult to acquire usable images during periods of maximum flooding. In addition, the technological evolution of Landsat sensors and the gradual increase in acquisition frequency over the decades have created an imbalance in the temporal density of observations. While recent periods (2013-2024) benefit from near-weekly coverage thanks to the complementary nature of the Landsat 7, 8 and 9 satellites, earlier decades have a much lower temporal resolution. This disparity potentially introduces a methodological bias in the comparison of hydrological statistics between different periods. Indeed, a higher acquisition frequency increases the probability of capturing short-lived flood peaks, which may artificially amplify the maximum values recorded during recent periods. To mitigate this bias, we have focused on analysing general trends and monthly composites rather than isolated instantaneous values, thus enabling a more robust comparison between the different periods despite their disparate temporal resolutions.

5.2. Hydrological Dynamics of the Yaéré and Control Factors

A diachronic analysis of the water surface in the Yaéré reveals a complex hydrological dynamic, characterised by high seasonal and inter-annual variability. The marked seasonal nature of the floods, with a peak in rainfall in September-October, corresponds to the rainfall regime and hydrological functioning of the Logone catchment.

This pattern is further clarified by the results shown in Figure 7, where it appears that heavy rainfall in August and September does not immediately translate into increased surface water extent. Instead, substantial expansion of flooded areas occurs from October onwards, indicating a delayed hydrological response largely governed by fluvial inputs. This surge in surface water is driven by the overflow of the Logone and Chari rivers, which discharge significant volumes into the Yaéré floodplain. These riverine contributions account for approximately 80%

of the total annual flooded area, compared to only 20% attributed to direct rainfall as shown by [20] [23]. Much of the early-season precipitation is either absorbed into dry soils or lost through evapotranspiration, as the initial rains primarily serve to recharge aquifers depleted by prolonged dry and hot conditions. Only once the soil moisture deficit is overcome does overland flow begin to manifest, enabling the accumulation of surface water and the onset of widespread inundation [23].

This flooding regime is fundamental to the Yaéré ecosystem, conditioning the biological productivity and ecosystem services associated with this vast floodplain. The inter-annual variability observed can be put into perspective with the regional climatic fluctuations documented by other studies. The years of low flooding (1984, 1987, 1988, 2007) coincide with periods of rainfall deficit reported in the literature for the Lake Chad basin [4] [14] [15] [28]. This flooding regime is fundamental to the Yaéré ecosystem, conditioning the biological productivity and ecosystem services associated with this vast floodplain. The inter-annual variability observed can be put into perspective with the regional climatic fluctuations documented by other studies. The years of low flooding (1984, 1987, 1988, 2007) coincide with periods of rainfall deficit reported in the literature for the Lake Chad basin. Conversely, years of exceptional flooding (1999, 2022, 2024) generally correspond to years of excess rainfall. These results confirm the hypothesis of the hydro system's high sensitivity to climatic forcing set out by [4]. Similarly, the results corroborate the observations of [35] on the Wuhan lake in China. The authors suggest that the dynamics of the surface states of Wuhan Lake are dependent on high precipitation and water conditions during the year.

The upward trend in maximum flooded areas since 2019, with all-time highs in 2022 (17,559 km^2) and 2024 (15,372 km^2), merits particular attention in the context of regional climate change characterised by an intensification of extreme precipitation. In a context characterised by a decrease in rainfall, [36] shows, on the basis of an examination of maps of water surfaces drawn up from Landsat images over a period of 30 years in the Haouz plain, a decline in water surfaces. The author identifies climate change, combined with strong population growth, as one of the factors contributing to the decline in water surface area, which is exerting strong pressure on surface water resources. This shows that anthropogenic changes to the hydrological system are also a determining factor in understanding the dynamics observed. The construction of the Maga dam and dykes along the Logone in the 1970s profoundly altered the natural flooding regime of the Yaéré. Faced with this worrying situation, a pilot reinundation trial was undertaken in May 1994, with the aim of restoring flooding in certain areas of the plain [25]. However, due to the absence of satellite data for this specific period, our results unfortunately do not allow us to directly assess the immediate impact of this intervention. Nevertheless, a comparison of the periods before 1990 and after 2000 suggests a potential improvement in hydrological conditions following this initiative, with a partial resumption of flooding in certain previously dry areas. Additional ecological studies have documented a gradual recolonisation of plant spe-

cies characteristic of flooded areas, confirming the relative effectiveness of this ecological restoration

6. Conclusions

This study analysed the hydrological dynamics of surface water in the Yaéré floodplain, situated in the Far North region of Cameroon, a vital wetland ecosystem within the Lake Chad basin characterised by its distinctive annual flood-recession cycle. The diachronic analysis spanning four decades reveals pronounced hydrological variability, with surface water extent ranging from complete absence (0 km^2) to a historical peak of 17,559 km^2 recorded in October 2022, and an average flooded area of around 1630 km^2.

The results highlight a marked seasonality in flooding, with flood maxima primarily occurring in September and October, consistent with the regional rainfall pattern and the hydrological regime of the Logone River. This seasonality is accompanied by strong interannual variability, with recent years (2019-2024) exhibiting an increase in exceptional flood events, potentially driven by intensified extreme rainfall episodes linked to broader climatic trends. These dynamics are further modulated by anthropogenic factors, notably the construction and operation of hydraulic infrastructures such as the Maga dam and Logone dikes, which have significantly altered the natural flood regime and spatial distribution of inundation.

Diachronic mapping of flooded areas has proven to be a valuable tool for detecting shifts in hydrological regimes and identifying zones of significant change. Such spatially explicit information is crucial for guiding ecological restoration efforts and for anticipating flood risks. While recent extreme floods may temporarily restore key ecological functions, they also pose considerable challenges for local communities in terms of flood risk management and socio-economic resilience.

Looking ahead, integrating additional satellite datasets, such as Sentinel-1 and Sentinel-2, will enhance the spatial and temporal resolution of surface water monitoring, particularly during the rainy season when optical imagery is hindered by cloud cover. Moreover, the application of advanced water detection techniques leveraging machine learning promises to improve the accuracy of flood mapping, especially in shallow and transient flood zones. Developing predictive hydrological models that couple observed water surface dynamics with regional climate projections will be essential to forecast future changes in this complex socio-ecological system, thereby supporting the design of effective, adaptive management and climate resilience strategies.

Conflicts of Interest

The authors declare no conflicts of interest regarding the publication of this paper.

References

[1] Bryzek, J.A., Veselka IV, W.E. and Anderson, J. (2024) State Role and Involvement

in Determining Wetland Mitigation Performance Standards in the United States. *Ecology and Society*, **29**, Article 30. https://doi.org/10.5751/es-14530-290130

[2] Sarwar Hossain, M. and Szabo, S. (2017) Understanding the Social-Ecological System of Wetlands. In: *Wetland Science*, Springer, 285-300. https://doi.org/10.1007/978-81-322-3715-0_15

[3] Bullock, A. and Acreman, M. (2003) The Role of Wetlands in the Hydrological Cycle. *Hydrology and Earth System Sciences*, **7**, 358-389. https://doi.org/10.5194/hess-7-358-2003

[4] Delclaux, F., Seignobos, C., Liénou, G. and Genthon, P. (2010) Water and People in the Yaéré Floodplain (North Cameroon). In: *Floodplains: Physical Geography, Ecology and Societal Interactions*, Nova Publishers, 1-27.

[5] Castellarin, A., Di Baldassarre, G. and Brath, A. (2011) Floodplain Management Strategies for Flood Attenuation in the River Po. *River Research and Applications*, **27**, 1037-1047. https://doi.org/10.1002/rra.1405

[6] Devitt, L., Neal, J., Coxon, G., Savage, J. and Wagener, T. (2023) Flood Hazard Potential Reveals Global Floodplain Settlement Patterns. *Nature Communications*, **14**, Article No. 2801. https://doi.org/10.1038/s41467-023-38297-9

[7] Jacobson, R.B., Lindner, G. and Bitner, C. (2015) The Role of Floodplain Restoration in Mitigating Flood Risk, Lower Missouri River, USA. In: *Geomorphic Approaches to Integrated Floodplain Management of Lowland Fluvial Systems in North America and Europe*, Springer, 203-243. https://doi.org/10.1007/978-1-4939-2380-9_9

[8] Ogawa, H. and Male, J.W. (1986) Simulating the Flood Mitigation Role of Wetlands. *Journal of Water Resources Planning and Management*, **112**, 114-128. https://doi.org/10.1061/(asce)0733-9496(1986)112:1(114)

[9] Acreman, M. and Holden, J. (2013) How Wetlands Affect Floods. *Wetlands*, **33**, 773-786. https://doi.org/10.1007/s13157-013-0473-2

[10] Guaita García, N., Martínez Fernández, J. and Fitz, C. (2020) Environmental Scenario Analysis on Natural and Social-Ecological Systems: A Review of Methods, Approaches and Applications. *Sustainability*, **12**, Article 7542. https://doi.org/10.3390/su12187542

[11] Lallemant, D., Hamel, P., Balbi, M., Lim, T.N., Schmitt, R. and Win, S. (2021) Nature-Based Solutions for Flood Risk Reduction: A Probabilistic Modeling Framework. *One Earth*, **4**, 1310-1321. https://doi.org/10.1016/j.oneear.2021.08.010

[12] Lloréns, J.L.P. (2008) Impacts of Climate Change on Wetland Ecosystems.

[13] Moritz, M., Laborde, S., Phang, S., Ahmadou, M., Durand, M., Fernandez, A., *et al.* (2016) Studying the Logone Floodplain, Cameroon, as a Coupled Human and Natural System. *African Journal of Aquatic Science*, **41**, 99-108. https://doi.org/10.2989/16085914.2016.1143799

[14] Scholte, P. (2005) Floodplain Rehabilitation and the Future of Conservation & Development. Adaptive Management of Success in Waza-Logone, Cameroon. Tropical Resource Management Papers.

[15] Sighomnou, D., Nkamdjou, L.S. and Liénou, G. (2002) La plaine du Yaéré dans le Nord-Cameroun: Une expérience de restauration des inondations. In: *Gestion intégrée des ressources naturelles en zones inondables tropicales*, IRD Éditions, 375-384. https://doi.org/10.4000/books.irdeditions.8565

[16] Raimond, C., Garine, É. and Langlois, O. (2013) Ressources vivrières et choix alimentaires dans le bassin du lac Tchad. IRD éditions.

[17] Westra, T. and De Wulf, R.R. (2009) Modelling Yearly Flooding Extent of the Waza-

Logone Floodplain in Northern Cameroon Based on MODIS and Rainfall Data. *International Journal of Remote Sensing*, **30**, 5527-5548. https://doi.org/10.1080/01431160802672872

[18] Ziébé, R. (2015) Fisheries in the Waza Logone floodplain: An Analysis of the Status of the Fisheries Sector and Mitigation of Conflicts within the Sector in North Cameroon. PhD Thesis, Leiden University.

[19] Béné, C., Neiland, A., Jolley, T., Ovie, S., Sule, O., Ladu, B., *et al.* (2003) Inland Fisheries, Poverty, and Rural Livelihoods in the Lake Chad Basin. *Journal of Asian and African Studies*, **38**, 17-51. https://doi.org/10.1177/0021909603038001002

[20] Fernández, A., Najafi, M.R., Durand, M., Mark, B.G., Moritz, M., Jung, H.C., *et al.* (2016) Testing the Skill of Numerical Hydraulic Modeling to Simulate Spatiotemporal Flooding Patterns in the Logone Floodplain, Cameroon. *Journal of Hydrology*, **539**, 265-280. https://doi.org/10.1016/j.jhydrol.2016.05.026

[21] Jung, H.C., Alsdorf, D., Moritz, M., Lee, H. and Vassolo, S. (2011) Analysis of the Relationship between Flooding Area and Water Height in the Logone Floodplain. *Physics and Chemistry of the Earth, Parts A/B/C*, **36**, 232-240. https://doi.org/10.1016/j.pce.2011.01.010

[22] Murumkar, A., Durand, M., Fernández, A., Moritz, M., Mark, B., Phang, S.C., *et al.* (2020) Trends and Spatial Patterns of 20th Century Temperature, Rainfall and PET in the Semi-Arid Logone River Basin, Sub-Saharan Africa. *Journal of Arid Environments*, **178**, Article 104168. https://doi.org/10.1016/j.jaridenv.2020.104168

[23] Naah, E. (1990) Hydrologie du grand Yaéré du nord Cameroun. Thèse de Doctorat es-sciences, Université de Yaoundé.

[24] Olivry, J.C. and Naah, E. (2000) Hydrologie. Atlas de La Province de l'Extrême Nord Du Cameroun, Paris, IRD.

[25] Loth, P.E. (2004) The Return of the Water: Restoring the Waza Logone Floodplain in Cameroon. IUCN.

[26] Labara, B.K., Djaowe, A., Tajo, D., Chouto, S., Chendjou, F.X. and Tagne, R. (2020) La pêche artisanale par canaux dans la plaine du Logone: Une rentabilité source de conflits entre pêcheurs. *Bulletin de la Société Géographique de Liège*, **75**, 83-100. https://doi.org/10.25518/0770-7576.6109

[27] Kolaouna Labara, B.K., Chouto, S. and Laborde, S. (2022) Des scénarios stratégiques pour une réflexion prospective sur les couplages écologiques et humains dans la plaine inondable du Logone (Extrême-Nord Cameroun). *Géographie et cultures*, **116**, 37-55.

[28] de Noray, M.L. (2002) Waza Logone: Histoires d'eaux et d'hommes; Vivre dans la plaine inondable de Waza Logone au Cameroun. IUCN.

[29] Mouafo, D., Fotsing, É., Sighomnou, D. and Sigha, L. (2002) Dam, Environment and Regional Development: Case Study of the Logone Floodplain in Northern Cameroon. *International Journal of Water Resources Development*, **18**, 209-219. https://doi.org/10.1080/07900620220121765

[30] Molenaar, J.W. and Van Santen, J.C.M. (2006) Perceptions of Water in a Changing Hydrological and Ecological Context: The Case of the Logone Flood Plains in Cameroon. *The Geographical Journal*, **172**, 331-347. https://doi.org/10.1111/j.1475-4959.2006.00216.x

[31] Gorelick, N., Hancher, M., Dixon, M., Ilyushchenko, S., Thau, D. and Moore, R. (2017) Google Earth Engine: Planetary-Scale Geospatial Analysis for Everyone. *Remote Sensing of Environment*, **202**, 18-27. https://doi.org/10.1016/j.rse.2017.06.031

[32] Olthof, I. and Fraser, R.H. (2024) Mapping Surface Water Dynamics (1985-2021) in

the Hudson Bay Lowlands, Canada Using Sub-Pixel Landsat Analysis. *Remote Sensing of Environment*, **300**, Article 113895.
https://doi.org/10.1016/j.rse.2023.113895

[33] Sakamoto, T., Van Nguyen, N., Kotera, A., Ohno, H., Ishitsuka, N. and Yokozawa, M. (2007) Detecting Temporal Changes in the Extent of Annual Flooding within the Cambodia and the Vietnamese Mekong Delta from MODIS Time-Series Imagery. *Remote Sensing of Environment*, **109**, 295-313.
https://doi.org/10.1016/j.rse.2007.01.011

[34] Funk, C., Peterson, P., Landsfeld, M., Pedreros, D., Verdin, J., Shukla, S., *et al.* (2015) The Climate Hazards Infrared Precipitation with Stations—A New Environmental Record for Monitoring Extremes. *Scientific Data*, **2**, Article No. 150066.
https://doi.org/10.1038/sdata.2015.66

[35] Deng, Y., Jiang, W., Tang, Z., Li, J., Lv, J., Chen, Z., *et al.* (2017) Spatio-Temporal Change of Lake Water Extent in Wuhan Urban Agglomeration Based on Landsat Images from 1987 to 2015. *Remote Sensing*, **9**, Article 270.
https://doi.org/10.3390/rs9030270

[36] El Halim, M. (2015) Apport de la télédétection pour l'évaluation de la variation des surfaces d'eau et du couvert végétal dans la plaine du Haouz depuis 1984 jusqu'à 2014. PFE, Université Cadi Ayyad.